NASA TECHNICAL NOTE

NASA TN D-2800

NASA TN D-2800

FACILITY FORM 602

N65-22607
(ACCESSION NUMBER)

22
(PAGES)

(NASA CR OR TMX OR AD NUMBER)

(THRU)

/
(CODE)

12
(CATEGORY)

EFFECT OF UNIFORM LONGITUDINAL STRAIN RATE ON WEAK HOMOGENEOUS TURBULENCE IN A COMPRESSIBLE FLOW

by Robert G. Deissler

Lewis Research Center

Cleveland, Ohio

NATIONAL AERONAUTICS AND SPACE ADMINISTRATION • WASHINGTON, D. C. • MAY 1965

NASA TN D-2800

EFFECT OF UNIFORM LONGITUDINAL STRAIN RATE ON WEAK HOMOGENEOUS TURBULENCE IN A COMPRESSIBLE FLOW

By Robert G. Deissler

Lewis Research Center
Cleveland, Ohio

NATIONAL AERONAUTICS AND SPACE ADMINISTRATION

For sale by the Clearinghouse for Federal Scientific and Technical Information
Springfield, Virginia 22151 – Price $1.00

EFFECT OF UNIFORM LONGITUDINAL STRAIN RATE ON WEAK HOMOGENEOUS TURBULENCE IN A COMPRESSIBLE FLOW

by Robert G. Deissler

Lewis Research Center

SUMMARY

22607

Two-point correlation equations for turbulence with a uniform strain rate in one direction are constructed by starting with the compressible Navier-Stokes and continuity equations. Compressibility is retained in the mean flow, but the problem is simplified by assuming that the turbulent eddies behave incompressibly. In order to close the system of equations, the weak turbulence approximation (triple correlations neglected) is used. The equations are converted to spectral form by taking their Fourier transforms. Solutions are obtained for the turbulent velocity variances in the longitudinal and transverse directions and for the spectra of those quantities. The transverse turbulent intensity (square root of variance over local mean velocity) varies in a complex manner that seems to approximate experimental heat transfer results in highly heated tubes.

A transfer term associated with the mean strain rate is found to transfer energy to either higher or lower wave numbers, depending on whether the strain rate is negative or positive. Because of this energy transfer the peaks of the energy and dissipation spectra are widely separated for large negative rates of strain, even though triple correlations have been neglected; however, there is still considerable overlap of the two spectra.

Author

INTRODUCTION

One problem of considerable interest in the theory of turbulent flow is the effect of a mean strain on the turbulence. Since the strain is accompanied by a velocity change in the flow direction, this effect is sometimes called an effect of acceleration. The case of turbulence with a suddenly applied mean strain, in which viscous and inertia effects produced by the turbulence are negligible, was considered, for instance, by Prandtl (ref. 1), Taylor (ref. 2), Ribner and Tucker (ref. 3), and Batchelor and Proudman (ref. 4). A different approach wherein viscous effects are retained and inertia effects are neglected only insofar as they affect triple correlations was used by Pearson (ref. 5). Two-point correlation equations in which uniform mean strain rates are included were obtained from the incompressible Navier-Stokes and continuity equations.

In the preceding analyses, a strain in the flow direction was accompanied by transverse strain, as in the distortion produced by a sudden stream contraction. The problem analyzed herein, on the other hand, considers the turbulence in a stream of uniform cross section, in which a uniform rate of strain is produced in the flow direction by density changes. This type of strain might be of importance in connection with heat transfer to or from a gas stream at high fluxes or in a flow with heat liberating or absorbing chemical reactions. The model might be closely approximated in an experiment in which a number of very small heated or cooled tubes run longitudinally in the stream. The turbulence would be initially produced by flow of the stream through a grid, and the effect of the strain rate on the decay of the turbulence would be studied.

The analysis starts from the compressible Navier-Stokes and continuity equations. From those equations two-point correlation equations for turbulence with a uniform mean rate of strain in one direction are obtained. Compressibility must, of course, be retained in the mean flow, but density fluctuations are neglected and the turbulent eddies are assumed to obey the incompressible continuity equation. The required correlation equations will be obtained in the following section.

BASIC EQUATIONS

The compressible Navier-Stokes and continuity equations for a constant-viscosity gas are usually written as follows:

$$\rho\left(\frac{\partial \tilde{u}_i}{\partial t} + \tilde{u}_k \frac{\partial \tilde{u}_i}{\partial x_k}\right) = -\frac{\partial \tilde{p}}{\partial x_i} + \frac{\mu}{3} \frac{\partial}{\partial x_i}\left(\frac{\partial \tilde{u}_k}{\partial x_k}\right) + \mu \frac{\partial^2 \tilde{u}_i}{\partial x_k \partial x_k} \tag{1}$$

and

$$\frac{\partial \rho}{\partial t} + \frac{\partial}{\partial x_k}(\rho \tilde{u}_k) = 0 \tag{2}$$

where the subscripts can take the values 1, 2, or 3. A repeated subscript in a term indicates a summation of terms, with the subscripts successively taking on the values 1, 2, and 3. The quantities $\tilde{u}_i$ and $\tilde{u}_k$ are instantaneous velocity components, x_i is a space coordinate, t is the time, ρ is the density, μ is the viscosity, and $\tilde{p}$ is the instantaneous pressure. (All symbols are defined in the appendix.)

Equations (1) and (2) give

$$\frac{\partial}{\partial t}(\rho \tilde{u}_i) + \frac{\partial}{\partial x_k}(\rho \tilde{u}_k \tilde{u}_i) = -\frac{\partial \tilde{p}}{\partial x_i} + \frac{\mu}{3} \frac{\partial}{\partial x_i}\left(\frac{\partial \tilde{u}_k}{\partial x_k}\right) + \mu \frac{\partial^2 \tilde{u}_i}{\partial x_k \partial x_k} \tag{3}$$

The instantaneous velocities and pressure in equations (3) and (2) can be broken into mean and fluctuating components. Set $\tilde{u}_i = U_i + u_i$, and $\tilde{p} = P + p$, where the capitalized symbols refer to mean quantities, and the lower case symbols refer to fluctuations. Density fluctuations are neglected.

If averages are taken and the averaged equations are subtracted from the unaveraged ones,

$$\frac{\partial}{\partial t}(\rho u_i) + \frac{\partial}{\partial x_k}(\rho U_i u_k) + \frac{\partial}{\partial x_k}(\rho U_k u_i) + \frac{\partial}{\partial x_k}(\rho u_i u_k) - \frac{\partial}{\partial x_k}(\rho \overline{u_i u_k})$$

$$= -\frac{\partial p}{\partial x_i} + \mu \frac{\partial^2 u_i}{\partial x_k \partial x_k} + \frac{\mu}{3}\frac{\partial}{\partial x_i}\left(\frac{\partial u_k}{\partial x_k}\right) \tag{4}$$

Since continuity is satisfied for the mean as well as for the unaveraged flow, equation (2) becomes

$$\frac{\partial \rho}{\partial t} + \frac{\partial}{\partial x_k}(\rho U_k) = 0 \tag{5}$$

Then, from equations (2) and (5),

$$\frac{\partial}{\partial x_k}(\rho u_k) = 0 \tag{6}$$

Also, since fluctuations are assumed to behave incompressibly, the incompressible continuity equation is used:

$$\frac{\partial u_k}{\partial x_k} \approx 0 \tag{7}$$

Comparison of this equation with equation (6) indicates that its use implies that changes in mean density are small over the distance for which a velocity fluctuation occurs. This distance can also be considered as the mixing length or scale of the turbulence or the distance over which velocities are appreciably correlated. Equation (7) allows dropping of the last term in equation (4). Use of equations (5) and (6) then gives

$$\rho \frac{\partial u_i}{\partial t} + \rho u_k \frac{\partial U_i}{\partial x_k} + \rho U_k \frac{\partial u_i}{\partial x_k} + \frac{\partial(\rho u_i u_k)}{\partial x_k} - \frac{\partial(\rho \overline{u_i u_k})}{\partial x_k} = -\frac{\partial p}{\partial x_i} + \mu \frac{\partial^2 u_i}{\partial x_k \partial x_k} \tag{8}$$

Equation (8) applies at a point P in the fluid. At another point P' separated from P by the vector $\vec{r}$ (see fig. 1),

$$\rho' \frac{\partial u_j'}{\partial t} + \rho' u_k' \frac{\partial U_j'}{\partial x_k'} + \rho' U_k' \frac{\partial u_j'}{\partial x_k'} + \frac{\partial(\rho' u_k' u_j')}{\partial x_k'} - \frac{\partial(\rho' \overline{u_j' u_k'})}{\partial x_k'} = -\frac{\partial p'}{\partial x_j'} + \mu \frac{\partial^2 u_j'}{\partial x_k' \partial x_k'} \tag{9}$$

If equation (8) is multiplied by $\rho' u_j'$ and equation (9) by ρu_i, the two equations are added, and average values are taken,

$$\rho\rho' \frac{\partial \overline{u_i u_j'}}{\partial t} + \rho\rho' \overline{u_k u_j'} \frac{\partial U_i}{\partial x_k} + \rho\rho' \overline{u_i u_k'} \frac{\partial U_j'}{\partial x_k'} + \rho\rho' U_k \frac{\partial \overline{u_i u_j'}}{\partial x_k}$$

$$+ \rho\rho' U_k' \frac{\partial \overline{u_i u_j'}}{\partial x_k'} + \frac{\partial(\rho\rho' \overline{u_i u_k u_j'})}{\partial x_k} + \frac{\partial(\rho\rho' \overline{u_i u_j' u_k'})}{\partial x_k'}$$

$$= -\rho' \frac{\partial \overline{p u_j'}}{\partial x_i} - \rho \frac{\partial \overline{u_i p'}}{\partial x_j'} + \rho'\mu \frac{\partial^2 \overline{u_i u_j'}}{\partial x_k \partial x_k} + \rho\mu \frac{\partial^2 \overline{u_i u_j'}}{\partial x_k' \partial x_k'} \tag{10}$$

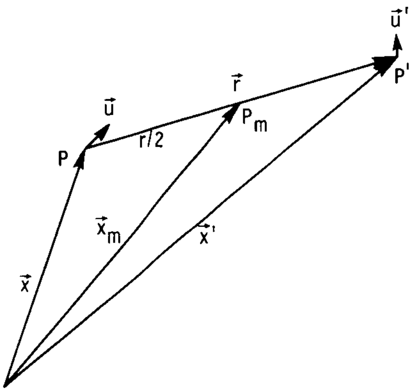

Figure 1. - Vector configuration for two-point correlation equations.

where the fact that quantities at one point are independent of the position of the other point has been used. As mentioned previously, use of the incompressible continuity equation for the fluctuations (eq. (7)) implies that changes in mean density are small over the distance for which velocities are correlated. Therefore, ρ' is replaced by ρ, and in that way a considerable simplification in equation (10) is obtained. Also, the turbulence is assumed to be weak enough for triple correlations to be neglected. Equation (10) then becomes, on introducing the new variables $r_k \equiv x_k' - x_k$ and $(x_k)_m \equiv (1/2)(x_k + x_k')$ (see fig. 1),

$$\frac{\partial \overline{u_i u_j'}}{\partial t} + \overline{u_k u_j'} \frac{\partial U_i}{\partial x_k} + \overline{u_i u_k'} \frac{\partial U_j'}{\partial x_k'} + \frac{U_k + U_k'}{2} \frac{\partial \overline{u_i u_j'}}{\partial (x_k)_m} + (U_k' - U_k) \frac{\partial \overline{u_i u_j'}}{\partial r_k}$$

$$= -\frac{1}{2\rho}\left[\frac{\partial \overline{p u_j'}}{\partial (x_i)_m} + \frac{\partial \overline{u_i p'}}{\partial (x_j)_m}\right] + \frac{1}{\rho}\left(\frac{\partial \overline{p u_j'}}{\partial r_i} - \frac{\partial \overline{u_i p'}}{\partial r_j}\right)$$

$$+ \frac{\mu}{2\rho} \frac{\partial^2 \overline{u_i u_j'}}{\partial (x_k)_m \partial (x_k)_m} + \frac{2\mu}{\rho} \frac{\partial^2 \overline{u_i u_j'}}{\partial r_k \partial r_k} \tag{11}$$

where the following transformations were used:

$$\frac{\partial}{\partial x_k} = \frac{1}{2} \frac{\partial}{\partial (x_k)_m} - \frac{\partial}{\partial r_k}$$

$$\frac{\partial}{\partial x_k'} = \frac{1}{2} \frac{\partial}{\partial (x_k)_m} + \frac{\partial}{\partial r_k}$$

For the problem considered herein, the velocity gradient (strain rate) in the x_1-direction dU_1/dx_1 is uniform, and the other velocity gradients are zero. Also, it is shown in reference 6 that the effects of inhomogeneities on the decay of the turbulence downstream of a grid are, for cases of practical interest, usually negligible. Equation (11) then becomes, for steady state at a given distance downstream from the turbulence generator,

$$\delta_{i1}\overline{u_1u_j'}\frac{\partial U_1}{\partial x_1} + \delta_{j1}\overline{u_iu_1'}\frac{\partial U_1}{\partial x_1} + (U_1)_m\frac{\partial\overline{u_iu_j'}}{\partial(x_1)_m} + \frac{\partial U_1}{\partial x_1}r_1\frac{\partial\overline{u_iu_j'}}{\partial r_1}$$

$$= \frac{1}{\rho}\left(\frac{\partial\overline{pu_j'}}{\partial r_i} - \frac{\partial\overline{u_ip'}}{\partial r_j}\right) + \frac{2\mu}{\rho}\frac{\partial^2\overline{u_iu_j'}}{\partial r_k\partial r_k} \tag{12}$$

where $(U_1 + U_1')/2$ was replaced by $(U_1)_m$, the value of U_1 at $(x_1)_m$, and δ_{ij} is the Kronecker delta.

The pressure-velocity correlations are next considered. Taking the divergence of equation (4) and using equations (6) and (7) give

$$\frac{\partial^2 p}{\partial x_i\partial x_i} = -2\frac{\partial^2(\rho U_iu_k)}{\partial x_k\partial x_i} - \frac{\partial^2(\rho u_iu_k)}{\partial x_k\partial x_i} + \frac{\partial^2(\rho\overline{u_iu_k})}{\partial x_k\partial x_i} \tag{13}$$

Since the mean flow is in the x_1-direction and changes only in the x_1-direction, the first term on the right side of equation (13) becomes, with the use of equations (5) and (7) and the assumption of steady state,

$$-2\frac{\partial}{\partial x_i}\left[u_k\frac{\partial(\rho U_i)}{\partial x_k}\right] = -2\frac{\partial}{\partial x_1}\left[u_1\frac{\partial(\rho U_1)}{\partial x_1}\right] = 0$$

Multiplying equation (13) by u_j', averaging, and introducing the variables $(x_i)_m$ and r_i then give, for weak turbulence,

$$\frac{1}{4}\frac{\partial^2\overline{pu_j'}}{\partial(x_i)_m\partial(x_i)_m} - \frac{\partial^2\overline{pu_j'}}{\partial(x_i)_m\partial r_i} + \frac{\partial^2\overline{pu_j'}}{\partial r_i\partial r_i} = 0 \tag{14}$$

Equation (14), however, is the same as equation (12) in reference 6. As in that reference $\overline{pu_j'}$ is assumed to be zero at an initial $(x_1)_m$. This assumption is consistent with an assumption to be made later that the turbulence is initially isotropic. In the preceding reference $\overline{pu_j'}$ is shown to be zero throughout the field if it is zero at an initial $(x_1)_m$; that is, the dynamics of the turbulence will not cause nonzero values of $\overline{pu_j'}$ to arise. Similarly, there will be no inconsistencies in also taking $\overline{u_ip'}$ to be zero. Equation (12) then becomes

$$\delta_{i1}\overline{u_1u_j'}\frac{\partial U_1}{\partial x_1} + \delta_{j1}\overline{u_iu_1'}\frac{\partial U_1}{\partial x_1} + (U_1)_m\frac{\partial\overline{u_iu_j'}}{\partial(x_1)_m} + \frac{\partial U_1}{\partial x_1}r_1\frac{\partial\overline{u_iu_j'}}{\partial r_1} = \frac{2\mu}{\rho}\frac{\partial^2\overline{u_iu_j'}}{\partial r_k\partial r_k} \tag{15}$$

In order to simplify the notation, let

$$(U_1)_m \equiv U \qquad \text{and} \qquad (x_1)_m \equiv x$$

By continuity,

$$\rho U = \rho_g U_g$$

or

$$\rho = \frac{\rho_g U_g}{U} \tag{16}$$

Also,

$$U = U_g + \frac{\partial U}{\partial x}x \tag{17}$$

where the subscript g designates the plane where $x = 0$ which, as usual, is taken as the plane of the grid. If

$$s \equiv \frac{\partial U_1}{\partial x_1} = \frac{\partial U}{\partial x} \tag{18}$$

$$X \equiv \frac{U_g}{s} + x \tag{19}$$

and

$$\nu \equiv \frac{\mu}{\rho_g}$$

equation (15) becomes

$$\delta_{i1}\overline{u_1u_j'} + \delta_{j1}\overline{u_iu_1'} + X\frac{\partial\overline{u_iu_j'}}{\partial X} + r_1\frac{\partial\overline{u_iu_j'}}{\partial r_1} = \frac{2\nu}{U_g}X\frac{\partial^2\overline{u_iu_j'}}{\partial r_k\partial r_k} \tag{20}$$

Equation (20) is the correlation equation for $\overline{u_iu_j'}$. It can be converted to spectral form by introducing the three-dimensional Fourier transform φ_{ij} defined by

$$\overline{u_i u_j'} = \int_{-\infty}^{\infty} \varphi_{ij} e^{i\vec{\kappa}\cdot\vec{r}} \, d\vec{\kappa} \tag{21}$$

where $d\vec{\kappa} = d\kappa_1 \, d\kappa_2 \, d\kappa_3$. Then,

$$r_1 \frac{\partial \overline{u_i u_j'}}{\partial r_1} = \int_{-\infty}^{\infty} - \left(\kappa_1 \frac{\partial \varphi_{ij}}{\partial \kappa_1} + \varphi_{ij}\right) e^{i\vec{\kappa}\cdot\vec{r}} \, d\vec{\kappa} \tag{22}$$

Taking the Fourier transform of equation (20) results in

$$U_g \frac{\partial \varphi_{ij}}{\partial X} = -\delta_{i1} \frac{U_g}{X} \varphi_{1j} - \delta_{j1} \frac{U_g}{X} \varphi_{i1} + \frac{U_g}{X}\left(\kappa_1 \frac{\partial \varphi_{ij}}{\partial \kappa_1} + \varphi_{ij}\right) - 2\nu\kappa^2 \varphi_{ij} \tag{23}$$

If X/U_g is interpreted as a time, the terms on the right side of equation (23) give the contributions of various processes to the time rate of change of φ_{ij}. The last term is, of course, the usual dissipation term. The next to the last term can be interpreted as a transfer term, for if $\vec{r} = 0$ in equation (22), the quantity $(\kappa_1 \, \partial\varphi_{ij}/\partial\kappa_1) + \varphi_{ij}$, when integrated over wave number space, gives zero contribution to the rate of change of $\overline{u_i u_j}$. It can, however, transfer energy between wave numbers. This process is similar to that previously discussed in connection with shear-flow turbulence (ref. 6). The remainder of the terms on the right side of equation (23) can evidently be interpreted as production terms. Both the production and transfer terms drop out of the equation when there is no strain, since X goes to infinity when s goes to zero (eq. (19)).

SOLUTION OF SPECTRAL EQUATION

Equation (23) is a first-order equation and can be solved by available methods (see ref. 7). For φ_{11}, the component of φ_{ij} in the direction of mean strain,

$$\varphi_{11} = \frac{f(\kappa_1 X)}{X} \exp\left[\frac{2\nu X}{U_g}\left(\kappa_1^2 - \kappa_2^2 - \kappa_3^2\right)\right] \tag{24}$$

where $f(\kappa_1 X)$ is a function of integration that depends on initial conditions. In order to evaluate f it is assumed that the turbulence is isotropic at $X = X_0$ (but not at other values of X). This assumption implies that, for weak turbulence,

$$\left(\varphi_{ij}\right)_0 = \frac{J_0}{12\pi^2}\left(\kappa^2 \delta_{ij} - \kappa_i \kappa_j\right) \tag{25}$$

where J_0 is a constant (see ref. 6, eq. (43)). This equation is in agreement with the work of Batchelor and Proudman (ref. 8). Evaluation of f in equation (24) by substituting equation (25) at $X = X_0$ gives

$$f(\kappa_1 X_0) = X_0 \frac{J_0}{12\pi^2}(\kappa_2^2 + \kappa_3^2)\exp\left\{-\frac{2\nu X_0}{U_g}\left[\frac{(\kappa_1 X_0)^2}{X_0^2} - \kappa_2^2 - \kappa_3^2\right]\right\}$$

or

$$f(\kappa_1 X) = \frac{J_0}{12\pi^2} X_0(\kappa_2^2 + \kappa_3^2)\exp\left[-\frac{2\nu X_0}{U_g}\left(\frac{\kappa_1^2 X^2}{X_0^2} - \kappa_2^2 - \kappa_3^2\right)\right]$$

Then

$$\varphi_{11} = \frac{J_0}{12\pi^2}\frac{U_g + sx_0}{U_g + sx}(\kappa^2 - \kappa_1^2)\exp\left\{-\frac{2\nu}{U_g}\kappa^2(x - x_0)\left[1 + s\left(\frac{\kappa_1}{\kappa}\right)^2 \frac{x - x_0}{U_g + sx_0}\right]\right\} \tag{26}$$

where the definition of x (eq. (19)) was used. Similarly, φ_{22}, a component normal to the direction of mean strain, is

$$\varphi_{22} = \frac{J_0}{12\pi^2}\frac{U_g + sx}{U_g + sx_0}\left[\kappa_3^2 + \kappa_1^2\left(\frac{U_g + sx}{U_g + sx_0}\right)^2\right]$$

$$\times \exp\left\{-\frac{2\nu}{U_g}\kappa^2(x - x_0)\left[1 + s\left(\frac{\kappa_1}{\kappa}\right)^2 \frac{x - x_0}{U_g + sx_0}\right]\right\} \tag{27}$$

Because of axial symmetry, φ_{33} is of the same form as φ_{22} and need not be considered separately.

In order to integrate over wave number space, it is convenient to introduce spherical coordinates as follows:

$$\left.\begin{aligned} \kappa_1 &= \kappa \cos\theta \\ \kappa_2 &= \kappa \cos\varphi \sin\theta \\ \kappa_3 &= \kappa \sin\varphi \sin\theta \end{aligned}\right\} \tag{28}$$

Equation (21) then becomes, for $\vec{r} = 0$,

$$\overline{u_i u_j} = \int_0^\infty \psi_{ij}\, d\kappa \tag{29}$$

where

$$\psi_{ij} = \int_0^{\pi} \int_0^{2\pi} \varphi_{ij} \kappa^2 \sin\,\theta\; d\varphi\; d\theta \tag{30}$$

The quantity ψ_{ij} is the spectrum tensor as defined by Batchelor (ref. 9).

In calculating $\overline{u_1^2}$ and $\overline{u_2^2}$ it is convenient to carry out the integration with respect to φ, κ, and θ in that order. Then, from equations (26) to (30),

$$\overline{u_1^2} = \frac{J_0}{48\sqrt{2\pi}} \left(\frac{U_g/\nu}{x - x_0}\right)^{5/2} \left(\frac{U_g + sx_0}{U_g + sx}\right)^{3/2} \tag{31}$$

and

$$\overline{u_2^2} = \overline{u_3^2} = \frac{J_0}{48\sqrt{2\pi}} \left(\frac{U_g/\nu}{x - x_0}\right)^{5/2} \frac{\left[s(x + x_0) + 2U_g\right](U_g + sx)^{1/2}}{2(U_g + sx_0)^{3/2}} \tag{32}$$

For the spectra of the velocity variances there is, in dimensionless form,

$$\psi_{11}^* = \frac{b\kappa^* e^{-2\kappa^{*2}}}{12\pi a} \left[\frac{(4a\kappa^{*2} - 1)}{4a} \sqrt{2\pi a}\ \mathrm{erf}\ (\kappa^* \sqrt{2a}) + \kappa^* e^{-2a\kappa^{*2}}\right] \tag{33}$$

and

$$\psi_{22}^* = \psi_{33}^* = \frac{\kappa^* e^{-2\kappa^{*2}}}{24\pi ab^3} \left\{\sqrt{2\pi a}\ \mathrm{erf}(\kappa^* \sqrt{2a}) \left[\frac{(b^2 - 2)(4a\kappa^{*2} - 1)}{4a} + 2\kappa^{*2}\right] + (b^2 - 2)k^* e^{-2a\kappa^{*2}}\right\} \tag{34}$$

for $a > 0$ and

$$\psi_{11}^* = \frac{b\kappa^* \exp\left[-2\kappa^{*2}(1 + a)\right]}{12\pi a} \left[\frac{4a\kappa^{*2} - 1}{\sqrt{-2a}} F(\sqrt{-2a}\ \kappa^*) + \kappa^*\right] \tag{35}$$

and

$$\psi_{22}^* = \psi_{33}^* = \frac{\kappa^* \exp\left[-2\kappa^{*2}(1 + a)\right]}{24\pi ab^3} \left[\frac{b^2(4a\kappa^{*2} - 1) + 2}{\sqrt{-2a}} F(\sqrt{-2a}\ \kappa^*) + (b^2 - 2)\kappa^*\right] \tag{36}$$

for $a < 0$, where

$$a = \frac{\frac{sx_0}{U_g}\left(\frac{x}{x_0} - 1\right)}{1 + \frac{sx_0}{U_g}} \tag{37}$$

$$b = \frac{1 + \frac{sx_0}{U_g}}{1 + \frac{sx}{U_g}} \tag{38}$$

$$\psi_{ij}^* = \psi_{ij} \frac{\nu^2(x - x_0)^2}{U_g^2 J_0} \tag{39}$$

$$\kappa^* = \left[\frac{\nu(x - x_0)}{U_g}\right]^{1/2} \kappa \tag{40}$$

$$\mathrm{erf}(\omega) = \frac{2}{\sqrt{\pi}} \int_0^{\omega} e^{-u^2}\, du \tag{41}$$

and

$$F(\omega) = e^{-\omega^2} \int_0^{\omega} e^{u^2}\, du \tag{42}$$

Values of $F(\omega)$ are tabulated, for instance, by Miller and Gordon (ref. 10).

The transfer term in the spectral equation (the next to the last term in eq. (23)) can be integrated over all directions in wave number space by replacing φ_{ij} in equation (30) by that term. The longitudinal component of the integrated transfer term is, then, in dimensionless form,

$$T_{11}^* = -\frac{b\kappa^* e^{-2\kappa^{*2}}}{12\pi a} \left[\frac{4a\kappa^{*2} - 3}{4a} \sqrt{2\pi a}\, \mathrm{erf}(\kappa^* \sqrt{2a}) + 3\kappa^* e^{-2a\kappa^{*2}}\right] + ab\psi_{11}^* \tag{43}$$

for $a > 0$ and

$$T_{11}^* = -\frac{b\kappa^* \exp[-2\kappa^{*2}(1 + a)]}{12\pi a} \left[\frac{4a\kappa^{*2} - 3}{\sqrt{-2a}} F(\sqrt{-2a}\, \kappa^*) + 3\kappa^*\right] + ab\psi_{11}^* \tag{44}$$

for $a < 0$, where

$$T_{11}^* = \frac{\nu^2(x - x_0)^3 s}{J_0 U_g^2(U_g + sx)} T_{11} \tag{45}$$

A discussion and plotting of the results for the various spectra and velocity variances will be given in the following section.

DISCUSSION

Velocity Variances

The velocity variances $\overline{u_1^2}$, $\overline{u_2^2}$, and $\overline{u_3^2}$ are given by equations (31) and (32). For zero strain ($s = 0$) these expressions reduce to the usual expression for isotropic turbulence in the final period, if $(x - x_0)/U_g = t - t_0$. In order to plot equations (31) and (32) for $s \neq 0$, the sign of x_0 must be known. It appears that x_0 must always be negative, since equations (31) and (32) indicate that the point $x = x_0$ represents a virtual origin for the turbulence, where the energy is infinite. Since the grid at $x = 0$ can produce only a finite turbulent energy, the virtual origin must lie upstream of the grid, or x_0 must be negative.

Dimensionless plots of equations (31) and (32) are presented in figure 2 for two values of x^*. The velocity variances at a given x with strain are divided by their values at the same position without strain, with the mean velocity set at U_g. For positive strain rates the longitudinal component $\overline{u_1^2}$ (in the direction of strain) is reduced below the value it would have for no strain, whereas the transverse components are increased. These results are qualitatively similar to those obtained for a sudden contraction in an incompressible flow (see ref. 9). For negative strain rates the opposite trends occur; that is, the longitudinal component is increased by the strain, whereas the transverse components are decreased. The total energy $\overline{u_i u_i}/2 = (\overline{u_1^2} + 2\overline{u_2^2})/2$ is increased by both positive and negative strain rates; that is, positive and negative strain rates both feed net energy into the turbulent field but through different components.

As $s^* x^*$ approaches -1 (or $sx \to -U_g$), $\overline{u_1^2}$ and thus $\overline{u_i u_i}$ grow indefinitely large (see eq. (31)). The symbols s^* and x^* are defined in figure 2. The point $sx = -U_g$ represents the condition where the fluid is compressed into zero volume and is, of course, unattainable.

For values of sx somewhat larger than $-U_g$, however, the magnitudes of $\overline{u_1^2}$ and $\overline{u_i u_i}$ still increase rather than decay as x increases, or the energy fed into the turbulent field by the negative straining action is greater than that dissipated. It can be shown from equation (31) that the region in which $\overline{u_1^2}$ increases with x is given by $-1/x^* < s^* < -(5/8)/[x^* + (3/8)]$.

Calculating the square of the transverse turbulent intensity $\overline{u_2^2}/U^2$, where U is the local mean velocity, is of some interest. In a sudden con-

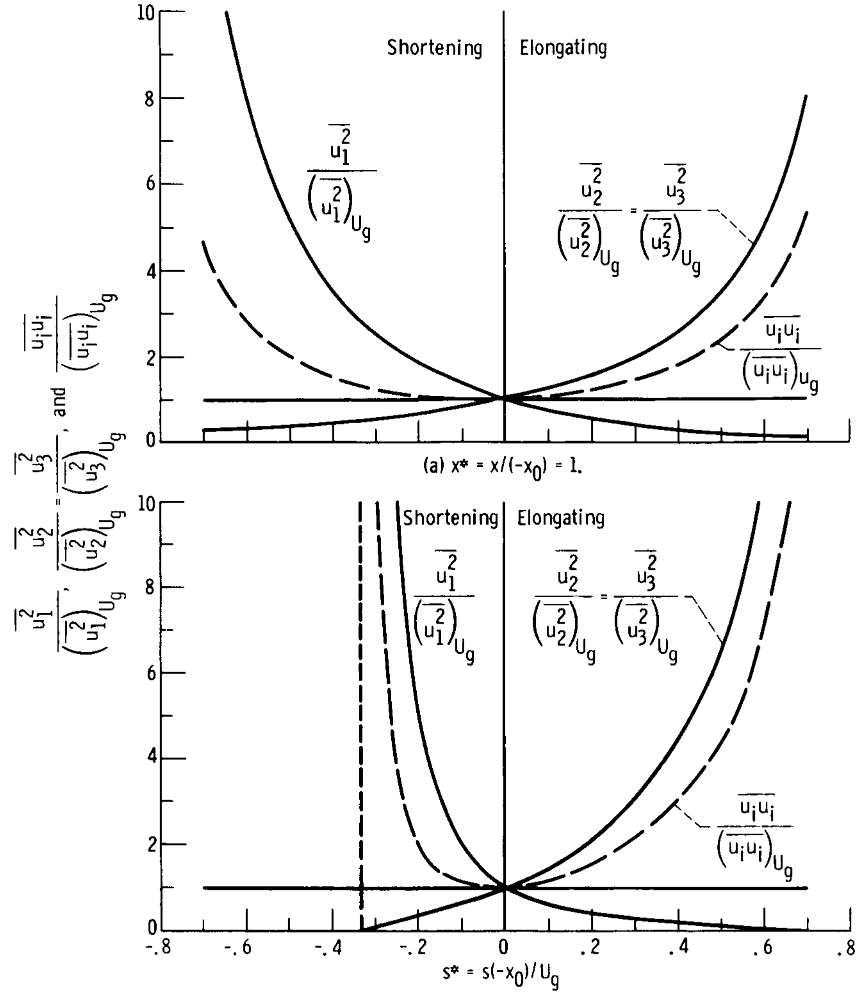

(a) $x^* = x/(-x_0) = 1$.

(b) $x^* = x/(-x_0) = 3$.

Figure 2. - Ratio of velocity variances with strain to those without strain as function of dimensionless mean strain rate.

traction, results for an incompressible flow indicate that, although $\overline{u_2^2}$ increases, $\overline{u_2^2}/U^2$ decreases through the contraction because of the increase in U (ref. 9). In the case presented herein it is desired to calculate

$$\frac{\left(\overline{u_2^2} \text{ at } x \text{ with strain}\right)\Big/\left(U^2 \text{ at } x \text{ with strain}\right)}{\left(\overline{u_2^2} \text{ at } x \text{ without strain and with } U = U_0\right)\Big/U_0^2}$$

or

$$\frac{\overline{u_2^2}/U^2}{\left(\overline{u_2^2}\right)_{U_0}\Big/U_0^2} = \frac{\overline{u_2^2}}{\left(\overline{u_2^2}\right)_{U_g}} \frac{\left(\overline{u_2^2}\right)_{U_g}}{\left(\overline{u_2^2}\right)_{U_0}} \left(\frac{U_0}{U}\right)^2 = \frac{\overline{u_2^2}}{\left(\overline{u_2^2}\right)_{U_g}} \left(\frac{U_g}{U_0}\right)^{5/2} \left(\frac{U_0}{U}\right)^2 = \frac{2 - s^*(1 - x^*)}{2(1 - s^*)^2(1 + s^* x^*)^{3/2}} \tag{46}$$

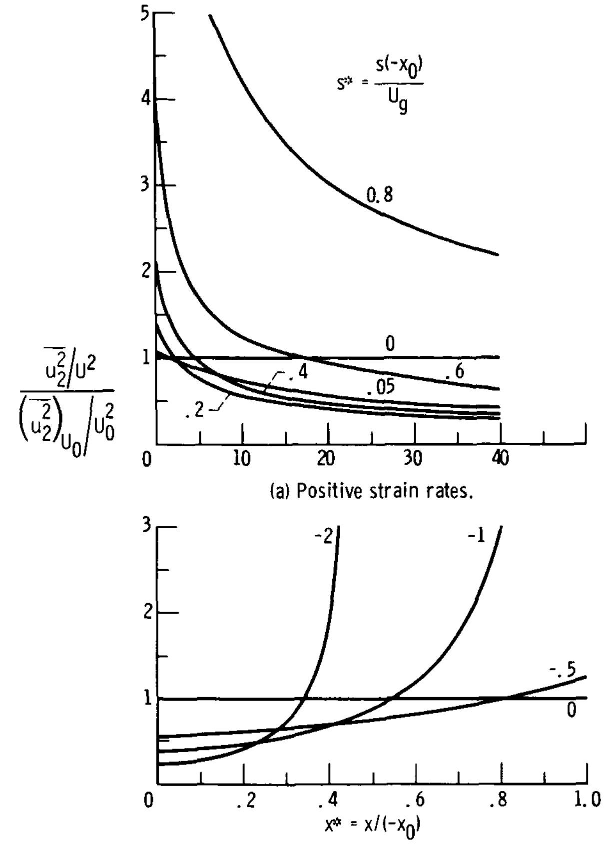

Figure 3. - Square of ratio of local transverse intensity of turbulence with strain to that without strain as function of dimensionless axial position and dimensionless strain rate.

where equation (32) and the relations $U = U_0 + s(x - x_0)$ and $U_g = U_0 - sx_0$ were used.

A plot of equation (46) is given in figure 3. For small values of x^* (fig. 3(a)), $\left(\overline{u_2^2}/U^2\right)\Big/\left[\left(\overline{u_2^2}\right)_{U_0}\Big/U_0^2\right]$ tends to be greater than 1 for positive strain; that is, the positive strain rate tends to increase the local transverse intensity of the turbulence. For larger values of x^*, the ratio is predominantly less than 1 except for large values of s^*. As x^* approaches infinity, equation (46) shows that the ratio of local transverse intensity with strain to that without strain goes to zero.

Comparing these results for positive strain rates with those for expanding flow in a highly heated tube may be worthwhile, although the heated-tube case is more complicated because of radial variations of velocities and properties. Experiments by Weiland (ref. 11; see fig. 7) and Taylor (ref. 12) indicate that the heat transfer in an expanding flow can be considerably different than might be expected for a nonexpanding flow. In the upstream portion of the tubes the heat-transfer coefficient tended to be higher than calculated for a normal entrance region. In the middle portion the heat-transfer coefficient dipped below the normal value, and near the exit of the longer tube it again rose. The experimental curves are qualitatively similar to those in figure 3(a), except that the latter do not rise near the exit. This difference can probably be attributed to the fact that the strain rate was not uniform along the length of the tube in the experiment. The dimensionless heat-transfer coefficient or Stanton number is closely related to the transverse turbulent intensity. In fact, some order of magnitude arguments based on the momentum - heat-transfer analogy can be used to show that the ordinate in figure 3 should be approximately proportional to the square of the ratio of local Stanton number with strain to that without strain. The results presented herein thus seem to be in qualitative agreement with the experimental heat-transfer results. Although, as mentioned previously, the heated-tube case is more complicated than the case considered herein, the results appear to show, at least, that appreciable effects of axial position on heat transfer at distances far downstream from the entrance might occur.

For negative strain rates (fig. 3(b)), the trends are, in general, opposite to those for positive strain rates; for small values of x^*,

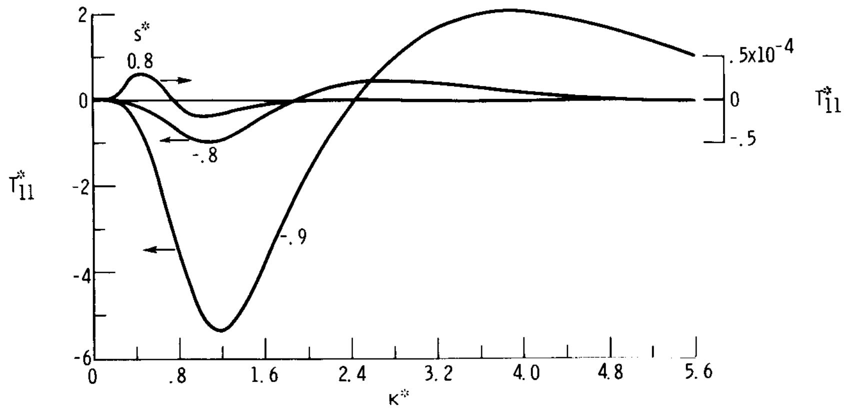

Figure 4. - Dimensionless longitudinal transfer spectra associated with mean strain at dimensionless axial position x^* of 1. (Arrows point to ordinate scales to be used for various curves.)

$\left(\overline{u_2^2}/U^2\right)\bigg/\left[\left(\overline{u_2^2}\right)_{U_0}\bigg/U_0^2\right]$ is less than 1, and for larger values of x^*, it becomes greater than 1. If the momentum - heat-transfer analogy is applied as it was for positive strain rates, it is seen that negative strain rates could either decrease or increase the heat-transfer coefficient. Negative strain rates occur, for instance, in the gas flowing through a cooled tube.

Turbulence Spectra

The dimensionless transfer spectra are next considered. The transfer term in the spectral equation for the longitudinal component of energy is plotted in figure 4 from equations (43) and (44). These curves and the succeeding ones are for a value of x^* of 1. Curves for other values of x^* are qualitatively similar. For negative strain rates the transfer term is negative for low values of κ^* and positive for large values, or the energy transfer is from small to large wave numbers. The total area under each curve as κ^* goes from zero to infinity is, of course, zero. The curves are similar to those obtained for the energy transfer associated with triple correlations at higher Reynolds numbers (ref. 13). In the case considered herein, where the triple correlations are neglected, the energy transfer is caused by the mean strain. For positive strain rates the energy transfer is in the opposite direction, that is, from large to small wave numbers. The energy transfer can thus be in either direction, depending on whether the strain rate is positive or negative. The transfer spectrum associated with the transverse energy, that is, the plot of T_{22}^*, although not shown, is similar to that of T_{11}^*, and the direction of the energy transfer corresponds to that for T_{11}^*.

Dimensionless spectra of the velocity variances, or values of ψ_{11}^* and ψ_{22}^*, are plotted in figures 5 and 6. For negative strain rates (figs. 5(a) and 6(a)), the shapes of the spectra are changed considerably because of the transfer of energy into the high wave number region as discussed in the preceding paragraph. The excitation of the high wave number portions of the spectra causes them to become asymmetric, as compared with the almost symmetric spectrum for no strain ($s^* = 0$). In the case of ψ_{22}^*, the curves for negative

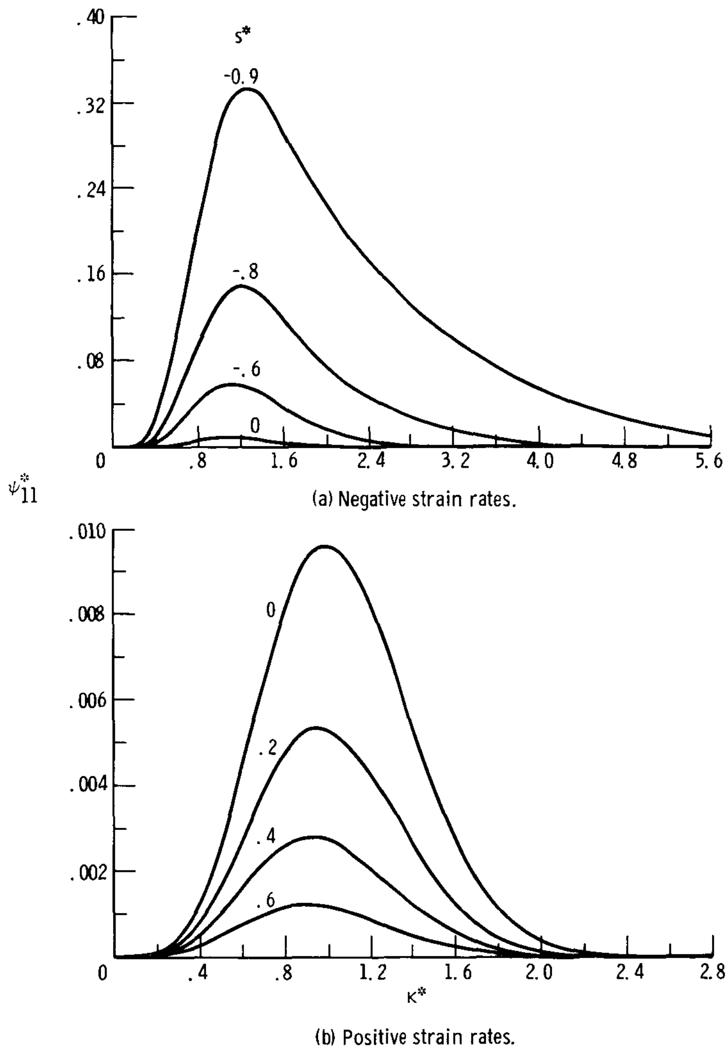

Figure 5. - Dimensionless longitudinal energy spectra at dimensionless axial position x^* of 1.

strain rates overlap because, although contributions to $\overline{u_2^2}$ with strain are generally lower than those without strain, the opposite trend occurs at high wave numbers because of the energy transfer into that region. For positive strain rates (figs. 5(b) and 6(b)), where the energy transfer is from large to small wave numbers, the shapes of the spectra are affected to a lesser extent by the energy transfer. Apparently, the effect of the energy transfer for positive strain rates is to move the peaks of the curves to the left, particularly those for ψ_{22}.

Figure 7 is a summary plot for energy, dissipation, and transfer spectra for a high negative strain rate ($s^* = -0.99$). The peaks of the energy and dissipation spectra are quite widely separated and occur at values of κ^* of 1.3 and 10, respectively. This separation is similar to the separation that occurs at high Reynolds numbers without mean strain (ref. 13) and is a consequence of the asymmetrical shape of the energy spectrum. The entire energy

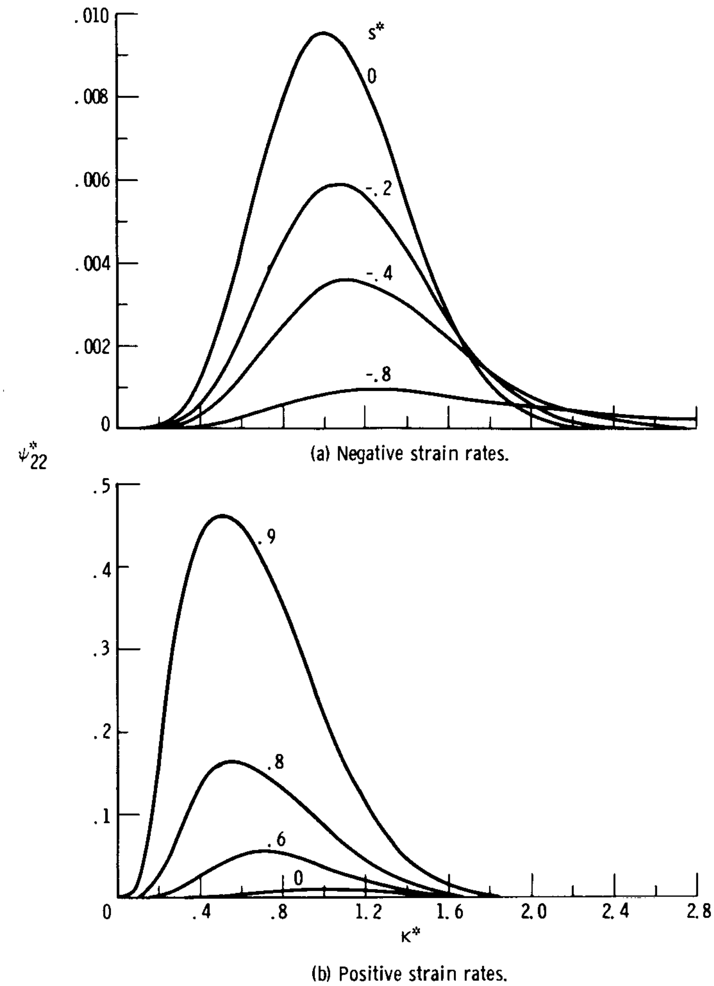

Figure 6. - Dimensionless transverse energy spectra at dimensionless axial position x^* of 1.

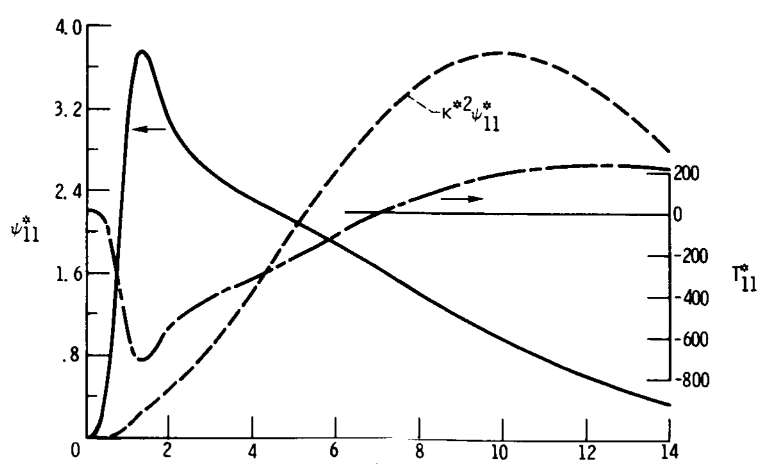

Figure 7. - Summary of longitudinal energy, dissipation, and transfer spectra for large negative strain rate (-0.99) at dimensionless axial position x^* of 1. (Peak of dissipation spectrum is normalized to same height as peak of energy spectrum.)

and dissipation regions, however, cannot be said to be widely separated, as is required for Kolmogoroff's hypothesis to be valid (see ref. 9) because there is considerable overlap of the spectra. In an attempt to obtain less overlap, a still higher value of negative strain rate ($s^* = -0.999$) was tried. Although the peak of the dissipation spectrum moved to about 32, while that of the energy spectrum was unchanged, the overlap of the regions was not decreased because ordinate values for the energy spectrum in the high wave number region were increased. It seems that a nearly complete separation of the energy and dissipation regions cannot be obtained with the present model.

Lewis Research Center,
National Aeronautics and Space Administration,
Cleveland, Ohio, February 17, 1965.

APPENDIX - SYMBOLS

a	defined by eq. (37)
b	defined by eq. (38)
F	defined by eq. (42)
J_0	constant that depends on initial conditions
P	mean pressure; also, a point in the fluid
p	pressure fluctuation
r	defined in fig. 1
s	$\frac{\partial U_1}{\partial x_1} = \frac{\partial U}{\partial x}$
T_{11}	longitudinal transfer term
t	time
$U,(U_1)_m$	mean longitudinal velocity component
u	velocity
X	$\frac{U_g}{s} + x$
$x,(x_1)_m$	longitudinal space coordinate
δ_{ij}	Kronecker delta
θ,φ	angular coordinates (see eq. (28))
κ	wave number
μ	viscosity
ν	μ/ρ_g
ρ	density
φ_{ij}	three-dimensional Fourier transform of $\overline{u_i u_j'}$ defined by eq. (21)
ψ_{ij}	spectrum tensor defined by eq. (30)

Subscripts:

g	at plane where $x = 0$ (plane of grid)
m	at point P_m (see fig. 1)

0 at virtual origin of turbulence where turbulent energy would be infinite (It is assumed that turbulence is isotropic at x_0 and that strain begins to act there.)

1 in longitudinal direction

2,3 in transverse direction

Superscripts:

~ instantaneous

' at point P' (see fig. 1)

* on dimensionless quantities defined by eqs. (39), (40), and (45)

REFERENCES

1. Prandtl, L.: Attaining a Steady Air Stream in Wind Tunnels. NACA TM 726, 1933.

2. Taylor, G. I.: Turbulence in a Contracting Stream. Zeitschr. f. Angew. Math. U. Mech. vol. 15, Feb. 1935, pp. 91-96.

3. Ribner, H. S.; and Tucker, M.: Spectrum of Turbulence in a Contracting Stream. NACA TN 2606, 1952.

4. Batchelor, G. K.; and Proudman, Ian: The Effect of Rapid Distortion of a Fluid in Turbulent Motion. Quart. J. Mech. and Appl. Math., vol. 7, 1954, pp. 83-103.

5. Pearson, J. R. A.: The Effect of Uniform Distortion on Weak Homogeneous Turbulence. J. Fluid Mech., vol. 5, pt. 3, 1959, pp. 274-288.

6. Deissler, Robert G.: Effects of Inhomogeneity and of Shear Flow in Weak Turbulent Fields. Phys. Fluids, vol. 4, no. 10, Oct. 1961, pp. 1187-1198.

7. Hildebrand, F. B.: Advanced Calculus for Engineers. Prentice-Hall, Inc., 1948, p. 374.

8. Batchelor, G. K.; and Proudman, I.: The Large-Scale Structure of Homogeneous Turbulence. Phil. Trans. Roy. Soc. (London), sec. A, vol. 248, no. 949, Jan. 5, 1956, pp. 369-405.

9. Batchelor, G. K.: The Theory of Homogeneous Turbulence. Cambridge Univ. Press, 1953.

10. Miller, W. L.; and Gordon, A. R.: Numerical Evaluation of Infinite Series and Integrals Which Arise in Certain Problems of Linear Heat Flow, Diffusion, etc. J. Phys. Chem., vol. 35, Oct. 1931, pp. 2785-2884.

11. Weiland, W. F.: Measurement of Local Heat Transfer Coefficients for Flow of Hydrogen and Helium in a Smooth Tube at High Surface to Fluid Bulk Temperature Ratios. Preprint 126, A.I.Ch.E., 1962.

12. Taylor, Maynard F.: Experimental Local Heat-Transfer and Average Friction Data for Hydrogen and Helium Flowing in a Tube at Surface Temperatures up to 5600° R. NASA TN D-2280, 1964.

13. Uberoi, Mahinder S.: Energy Transfer in Isotropic Turbulence. Phys. Fluids, vol. 6, no. 8, Aug. 1963, pp. 1048-1056.

NASA-Langley, 1965 E-2835